

Turret-Runner-Penetrator Differential Game with Role Selection

Alexander Von Moll^{1,2}, Daigo Shishika³, Zachariah Fuchs², and Michael Dorothy⁴

Abstract—A scenario is considered in which two cooperative Attackers aim to infiltrate a circular target guarded by a Turret. The engagement plays out in the two dimensional plane; the holonomic Attackers have the same speed and move with simple motion and the Turret is stationary, located at the target circle’s center, and has a bounded turn rate. When the Turret’s look angle is aligned with an Attacker, that Attacker is neutralized. In this paper, we focus on a region of the state space wherein only one of the Attackers is able to reach the target circle – and even then, only with the help of its partner Attacker. The Runner distracts the Turret until it is neutralized, which allows the Penetrator to gain a positional advantage and guarantee success in hitting the target circle. We formulate the Turret-Runner-Penetrator scenario as a differential game over the Value of the subsequent game of min/max terminal angle which takes place between the Turret and Penetrator once the Runner has been neutralized. The solution to the Game of Degree, including equilibrium Turret, Runner, and Penetrator strategies, as well as the Value function are given. The case in which the Penetrator can reach the target before the Turret can neutralize the Runner is formulated and solved. Finally, the assumption of *a priori* defined roles/goals is relaxed and the minimum of the solutions to the two fixed-role games is shown to be a Global Stackelberg Equilibrium.

I. INTRODUCTION

Cooperation is essential for success in conflicts between teams of agents. Certain outcomes are only possible through cooperation; victory could even be contingent on the sacrifice of a particular agent. In this paper, we consider a cooperative team of Attackers who seek to collide with a static target that is guarded by a Turret. The Turret is equipped with a directional weapon which can be aimed (turned) with bounded rate. When the Turret’s look angle is aligned with the position of an Attacker, that Attacker is considered to be neutralized. Our focus is on providing a rigorous solution for the case where there are two Attackers. This is a step towards analyzing the defense of a static location or asset against “swarms” of Attackers with a directional defensive weapon. In particular, we aim

We gratefully acknowledge the support of ARL grant DCIST CRA W911NF-17-2-0181.

The views expressed in this paper are those of the authors and do not reflect the official policy or position of the United States Air Force, United States Army, Department of Defense, or the United States Government.

¹Control Science Center of Excellence, Air Force Research Laboratory, 2210 8th St. WPAFB, OH 45433 alexander.von_moll@us.af.mil

²Department of Electrical Engineering and Computing Systems, University of Cincinnati, Cincinnati, OH 45221

³Department of Mechanical Engineering, George Mason University, Fairfax, VA 22030

⁴Combat Capabilities Development Command, Army Research Laboratory, Adelphi, MD, 20783

Manuscript received MMM DD 2021; revised MM DD 2022

to consider the many Attacker case wherein the Turret must destroy all (or as many as is possible) Attackers in succession; the Attackers, meanwhile, coordinate their attack to maximize successful hits. With the prospective proliferation of lower-cost unmanned vehicles and guided munitions, solving this problem is of interest, both from the attackers’ and defender’s perspective. See, for example, the following excerpt from the Air Force 2030 Science & Technology Strategy document [1] (emphasis added):

Swarms of low-cost, autonomous air and space systems can ... **absorb losses** that manned systems cannot... Low-end systems can restore the agility to attack adversary weaknesses in unexpected ways by **exploiting numbers** and complexity.

Various turret and turret-like defense scenarios have been explored in recent literature. These scenarios may be considered to be a subclass of target guarding (c.f. [2]–[4]), or even more generally, reach-avoid problems (e.g., [5], [6]).

The works vary in aspects such as number of agents, cost functional (particularly integral versus terminal), and termination conditions. However, the agents’ kinematics are essentially the same with the slight exception of the Turret/Defender. In some cases, the Defender is modeled as an agent with bounded speed who is constrained to move along the perimeter of the target circle, and in others, the Defender is stationary and turn-constrained Turret; these two models are equivalent. In [7], the authors formulated and solved the Turret Defense Differential Game (along with all of its singularities) wherein the cost functional included a state-dependent integral cost. There, a single mobile Attacker sought to balance time-to-target with avoiding the line of sight of the Turret; the resulting Attacker trajectories are generally curved in the Cartesian frame. Reference [8] analyzed a perimeter patrol scenario wherein termination occurs either when the Attacker reaches the target or when the Defender and Attacker are coincident. The solution characteristics of the single-Attacker, single-Defender and single-Attacker, two-Defender scenarios were then extended to a many-Attacker, many-Defender variant wherein the teams maximize (minimize, respectively) the number of hits on the target. An extension considered a heterogeneous Defender team comprised of uncontrolled and controlled patrollers [9]. In [10], [11], the authors solved a similar scenario but with turret-style termination conditions (i.e. line of sight neutralization) for the single-Attacker, single-Turret and single-Attacker, two-Turret cases. This paper is an extension thereof in which we consider aspects of the two-Attacker, single-Turret case.

We consider a particular sub-case wherein one of the Attackers must sacrifice itself in order for the other Attacker to reach the target unhindered. Because the Attackers essentially have different roles, this problem is also related to other “three-body” problems in the literature, such as the Target Attacker Defender Differential Game [12], [13]. There, the Defender/Target team seek to cooperatively maneuver in such a way for the Defender to intercept the Attacker as far from the Target as possible. Another example is the single-pursuer, two-evader cooperative defense scenario presented in [14] wherein one of the Evaders performs a flanking maneuver on the Pursuer to drive up the Pursuer’s cost. The work in this paper is also related to the problem of capture of evaders in succession [6], [15]–[17] since the Turret is free to aim at another Attacker once one is neutralized. The role selection portion of the analysis pertains to the determination of which Attacker will be pursued by the Turret first thereby fixing that Attacker to be the sacrificial one. This type of question (i.e., whether to behave as a ‘Runner’ or ‘Penetrator’) appears elsewhere in the differential game literature. For example, whether to behave as the Pursuer or Evader in symmetric engagements [18], e.g., the Game of Two Cars [19], [20], and in [21]. Other examples include the determination of which agent is the leader and which is the follower, as in the cooperative Homicidal Chauffeur game studied in [22].

The two-Attacker, single-Turret problem is formulated and solved (for a particular region of the state space) using the framework of differential game theory (c.f. [2]). In particular, we address the case in which neither Attacker can guarantee to reach the target individually, but, through their cooperation, the Attackers can guarantee that one can. We thus pose and solve the Turret-Runner-Penetrator Differential Game (TRPDG), providing both the Value function and equilibrium strategies. Within the TRPDG, we consider the case where the Runner is neutralized before the Penetrator reaches the target, and the case where the Penetrator reaches the target first. This work extends [23] by solving the latter case and also addressing the case where the Attackers’ roles are undetermined and the Turret is allowed to switch. Section II provides a formulation for the overall two-Attacker, single-Turret problem and breaks the general problem up based on how many Attackers can be guaranteed to reach the target. Section III specifies the TRPDG with Runner neutralization which takes place in the state space region where exactly one Attacker can be guaranteed to reach the target; this version of the game ends when the Runner is neutralized. Section IV provides a formulation and solution for the TRPDG with early penetration; in this version of the game, the Penetrator reaches the target circle before the Runner is neutralized. Section V considers the case where the Turret is allowed to choose either Attacker to pursue (at any time). Section VII provides some conclusions and identifies specific problems to address in future work.

II. PROBLEM FORMULATION

In general, there are two scenarios one may consider: upon an Attacker’s arrival to the target circle 1) the Turret is destroyed or 2) the Turret is not destroyed. We focus on

the latter scenario. Concerning a measure of performance, there are two obvious metrics that may be considered: time (e.g., time to neutralize, time to penetrate, etc.) or angular separation (i.e., at the time of penetration), either of which are perfectly valid. The former makes sense if, for example, the Attackers represent some kind of munition and thereby angular separation is not as critical. Meanwhile, the latter may make sense if the Attackers represent intruders that have secondary objectives upon reaching the target circle. Both metrics are considered, e.g., in [11]. In this paper we consider angular separation to be the metric of interest.

In this formulation, the speed of the two Attackers are equal. Without loss of generality, the Turret’s maximum turn rate and the target circle radius are normalized to be 1 according to the time and distance scaling presented in [10]. Let $\nu < 1$ be the ratio of the Attackers’ speed and Turret’s maximum turn rate. Let $\hat{\mathbf{z}} = (x_R, y_R, x_P, y_P, \beta)$ be the state of the system wherein the two Attackers’ positions are represented by their 2-D Cartesian coordinates and the Turret’s look angle is β w.r.t. the positive x -axis. The subscript R denotes Runner, and the subscript P denotes Penetrator. The kinematics are thus

$$\hat{f}(\hat{\mathbf{z}}) = \begin{bmatrix} \dot{x}_R \\ \dot{y}_R \\ \dot{x}_P \\ \dot{y}_P \\ \dot{\beta} \end{bmatrix} = \begin{bmatrix} \nu \cos \hat{\psi}_R \\ \nu \sin \hat{\psi}_R \\ \nu \cos \hat{\psi}_P \\ \nu \sin \hat{\psi}_P \\ u_T \end{bmatrix}, \quad (1)$$

where $\hat{\psi}_R, \hat{\psi}_P$ are the Attackers’ headings measured w.r.t. the positive x -axis, and $u_T \in [-1, 1]$ is the Turret’s angular velocity input (with positive u_T corresponding to counter-clockwise motion). Alternatively, the Attackers’ positions may be expressed in a polar coordinate system centered on the target circle’s center. Define $\mathbf{z} = (r_R, \theta_R, r_P, \theta_P, \beta)$ where θ_R, θ_P are measured relative to the Turret’s look angle. Also let $A_R \equiv (r_R, \theta_R)$ and $A_P \equiv (r_P, \theta_P)$; the Turret is also denoted T. The associated kinematics are

$$f(\mathbf{z}) = \begin{bmatrix} \dot{r}_R \\ \dot{\theta}_R \\ \dot{r}_P \\ \dot{\theta}_P \\ \dot{\beta} \end{bmatrix} = \begin{bmatrix} -\nu \cos \psi_R \\ \frac{\nu}{r_R} \sin \psi_R - u_T \\ -\nu \cos \psi_P \\ \frac{\nu}{r_P} \sin \psi_P - u_T \\ u_T \end{bmatrix}, \quad (2)$$

where ψ_R, ψ_P are measured clockwise w.r.t. the line from the respective Attacker to the target circle center. Figure 1 depicts the scenario, showing both coordinate systems specified above.

An Attacker A_i is considered to be neutralized (and removed from the remainder of the ployout, if any) if at any time $\theta_i = 0$. Conversely, A_i is said to penetrate the target if it can maneuver all the way to the target circle ($r_i = 1$) while avoiding the Turret’s line-of-sight. Ideally, both Attackers would like to penetrate the target without being neutralized.

In the general case, there are three termination cases: (i) both Attackers penetrate the target, (ii) one Attacker is neutralized and one penetrates, or (iii) both Attackers are neutralized. Cases (i) and (iii) are discussed briefly in the Appendix. The remainder of the paper focuses on the state

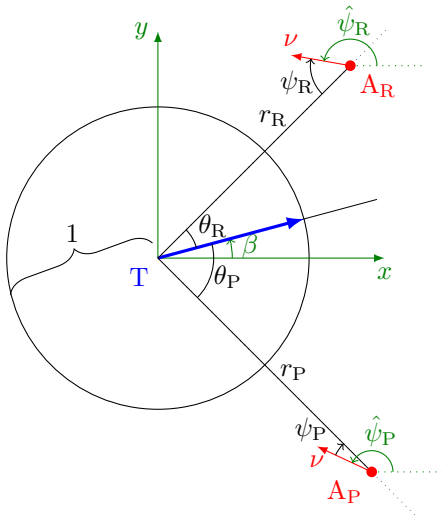


Fig. 1. Two Attacker Scenario – the green color indicates the Cartesian coordinate system; black represents the polar coordinate system. The Attacker position angles, θ_R and θ_P , are measured w.r.t. T's look angle and are positive in the CCW direction (thus $\theta_P < 0$, as shown).

space region wherein $A_R, A_P \notin \mathcal{R}_A$ at initial time, where \mathcal{R}_A is the single-Attacker, single-Turret Attacker's win region, defined in (47) in the Appendix. This is the region in which a single Attacker can be guaranteed to penetrate the target. When $A_R, A_P \notin \mathcal{R}_A$, neither Attacker can guarantee successful penetration of the target by itself; we will construct a subset of this region in which, through their cooperation and superiority in numbers, one of the Attackers can successfully penetrate. Let the region of interest for this state space be defined as

$$\Omega := \{z \mid A_R, A_P \notin \mathcal{R}_A, r_R, r_P \geq 1\}. \quad (3)$$

As mentioned previously, angular separation is the metric of interest, therefore, when it is possible for the Penetrator to reach the target, the cost functional takes the form

$$J(z; u_T(\cdot), \psi_R(\cdot), \psi_P(\cdot)) = |\theta_P(t_f)|. \quad (4)$$

The overall scenario may be broken down into two phases. In Phase 1, without loss of generality, the Turret pursues A_R until its aim is aligned with A_R 's position, at which time A_R is taken out of action. Thereby, Phase 2 commences, wherein the Turret begins pursuing A_P . Figure 2 depicts these two phases.

It may also be the case that the A_P is able to reach the target circle prior to A_R 's demise, whereby $t_f \leq t_c$. In this case, there is no Phase 2. We refer to this case as the Early Penetrator (EP) case. We analyze the case depicted in Fig. 2 in the following section, and the Early Penetrator is the focus of Section IV. Both of these cases fall under what we refer to as the Turret-Runner-Penetrator Differential Game (TRPDG).

III. TRPDG WITH RUNNER NEUTRALIZATION

In this section we construct a differential game representing Phase 1 in Fig. 2 wherein we assume that T neutralizes A_R (before A_P is able to penetrate the target). We proceed with the analysis in the polar coordinate system, utilizing (2), with

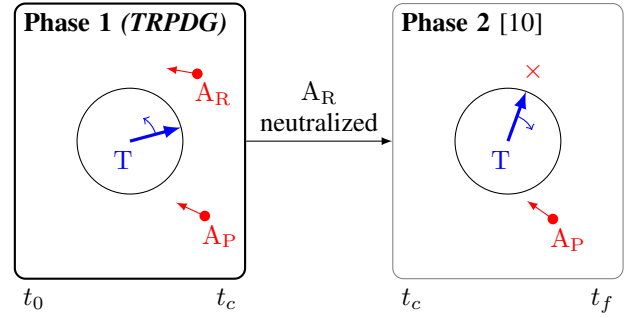


Fig. 2. Abstract depiction of the scenario; in Phase 1 T pursues A_R while A_P seeks advantageous position for Phase 2, and Phase 2 is the remaining single-Attacker *Game of Angle*.

$z \in \Omega$. A major assumption is made at this point, which is that the fate (goals and roles) of each Attacker is set *a priori*; and, moreover, these roles cannot be switched during the playout of the game. Let A_R be the first Attacker to be neutralized by T, regardless of the position of A_P . A complete solution, which involves the agents determining which Attacker T will pursue and neutralize first, necessarily depends on the solution of this simpler problem. This restriction is also motivated by some real-world considerations: often it is costly for a weapon (or targeting) system to switch targets after it has begun tracking a particular target.

Concerning the control signals u_T , ψ_R , and ψ_P , it is assumed that the agents have full state information (i.e., z is known) but they do not know the instantaneous control of the adversary. That is, neither T nor A_R, A_P are discriminated. In general, the solution approach utilized throughout the remainder of the paper, which is based on the formation of the first-order necessary conditions for equilibrium, yields an open-loop equilibrium [24, pg. 344]. From the open-loop solution, the closed-loop (state-feedback) strategies may be synthesized [24, pg. 344]. In order to constitute an equilibrium, the proposed strategies would need to satisfy the sufficient conditions (i.e., yield a Value function that is C^1 and satisfy the Hamilton-Jacobi-Isaacs equation) – however, these conditions will be satisfied by construction everywhere except for the singularities. Thus special attention is given to these singularities to ensure the validity of the solution.

We begin by assuming that A_P can reach the target circle ($r_P(t_f) = 1$) in Phase 2 (c.f. Fig. 2) and that A_P prefers to maximize its angular separation from T at final time. That is, in the second phase of the engagement that begins when A_R is neutralized, A_P plays the *Game of Angle* (a *Game of Degree* over the terminal θ_P), as specified in [10]. As such, we refer to A_R as the Runner, and A_P as the Penetrator. Define the region in which A_P can reach the target circle in Phase 2 as

$$\mathcal{R}_{2A} \equiv \{z \mid A_P(t_c) \in \mathcal{R}_A\}. \quad (5)$$

The explicit construction and solution of a *Game of Degree* wherein A_P is also neutralized is left for future work. We model the *first* phase of the engagement as a zero-sum

differential game over the cost functional

$$\begin{aligned} J(\mathbf{z}; u_T(\cdot), \psi_R(\cdot), \psi_P(\cdot)) &= \Phi(\mathbf{z}(t_c), t_c) \\ &= V_{AP}(r_P(t_c), \theta_P(t_c)), \end{aligned} \quad (6)$$

where $\mathbf{z} \in \mathcal{R}_{2A}$ and V_{AP} is the Value of the *Game of Angle* (i.e., the single-Attacker game, studied in [10]) played between A_P and T starting from $t = t_c$, and t_c is the terminal time of the game, which occurs when A_R is neutralized. Eq. (6) is related to (4) in that by employing equilibrium strategies in Phase 1, T and A_P set themselves up for the best possible outcome in Phase 2 with regards to $|\theta_P(t_f)|$. We define the terminal manifold as

$$\phi(\mathbf{z}(t_c), t_c) = \theta_R(t_c) = 0. \quad (7)$$

The Attackers cooperatively seek to maximize J , while the Turret wants to minimize J . Thus the Value function for the TRPDG with Runner neutralization is defined as

$$V(\mathbf{z}) = \min_{u_T(\cdot)} \max_{\psi_R(\cdot), \psi_P(\cdot)} J(\mathbf{z}; u_T(\cdot), \psi_R(\cdot), \psi_P(\cdot)). \quad (8)$$

The Value function of the *Game of Angle* is given in [10] as

$$V_{AP}(r_P, \theta_P) = |\theta_P| - \theta_{GOK}(r_P), \quad (9)$$

where θ_{GOK} is the single-Attacker, single-Turret *Game of Kind* surface defined in (48) in the Appendix. Figure 2 depicts the overall scenario broken up into two distinct phases: Phase 1, which terminates at $t = t_c$ when A_R is neutralized, and Phase 2 wherein A_P and T play out the *Game of Angle*. The Value function, V_{AP} , of Phase 2 determines, in part, the equilibrium strategies in Phase 1.

We use the notation $\mathbf{z}_c \equiv \mathbf{z}(t_c)$ generally. The Hamiltonian is

$$\mathcal{H} = \lambda_\beta u_T + \sum_{i=R,P} -\lambda_{r_i} \nu \cos \psi_i + \lambda_{\theta_i} \left(\frac{\nu}{r_i} \sin \psi_i - u_T \right). \quad (10)$$

The equilibrium adjoint dynamics are [25]

$$\dot{\boldsymbol{\lambda}} = -\frac{\partial \mathcal{H}}{\partial \mathbf{z}} = \begin{bmatrix} -\frac{\nu}{r_R^2} \lambda_{\theta_R} \sin \psi_R \\ 0 \\ -\frac{\nu}{r_P^2} \lambda_{\theta_P} \sin \psi_P \\ 0 \\ 0 \end{bmatrix}, \quad (11)$$

and thus λ_{θ_R} , λ_{θ_P} , and λ_β are constant. The transversality condition yields the adjoint values at terminal time [25]

$$\begin{aligned} \boldsymbol{\lambda}_c^\top &= \frac{\partial \Phi}{\partial \mathbf{z}_c} + \mu \frac{\partial \phi}{\partial \mathbf{z}_c} \\ &= \begin{bmatrix} 0 & 0 & \frac{\partial V_{AP}}{\partial r_P} & \frac{\partial V_{AP}}{\partial \theta_P} & 0 \end{bmatrix} + \mu \begin{bmatrix} 0 & 1 & 0 & 0 & 0 \end{bmatrix}. \end{aligned} \quad (12)$$

Let the adjoints of A_P 's single-Attacker *Game of Angle* [10] be written

$$\boldsymbol{\sigma}^\top \equiv [\sigma_r \quad \sigma_\theta] = \left[\frac{\partial V_{AP}}{\partial r_P} \quad \frac{\partial V_{AP}}{\partial \theta_P} \right].$$

Notice that $\lambda_{\beta_c} = 0$ and $\dot{\lambda}_\beta = 0$, thus $\lambda_\beta = 0$ for all $t \in [0, t_c]$. Similarly, $\lambda_{\theta_R} = \mu$ and $\lambda_{\theta_P} = \sigma_\theta$ for all $t \in [0, t_c]$.

Substituting the values of λ_β , λ_{θ_R} , and λ_{θ_P} , the Hamiltonian becomes

$$\begin{aligned} \mathcal{H} &= -\lambda_{r_R} \nu \cos \psi_R + \mu \left(\frac{\nu}{r_R} \sin \psi_R - u_T \right) \\ &\quad - \lambda_{r_P} \nu \cos \psi_P + \sigma_\theta \left(\frac{\nu}{r_P} \sin \psi_P - u_T \right). \end{aligned} \quad (13)$$

The Hamiltonian is a separable function of the controls u_T and ψ_R, ψ_P , and thus *Isaacs' condition* [2], [24] holds:

$$\min_{u_T} \max_{\psi_R, \psi_P} \mathcal{H} = \max_{\psi_R, \psi_P} \min_{u_T} \mathcal{H}.$$

The following result applies generally to differential games based on these dynamics with a well-defined terminal cost functional and terminal surface; it arises mainly as a consequence of the fact that the Attackers have simple motion (i.e., single integrator dynamics). Most of the later results in this paper rely heavily on the following:

Lemma 1 (Equilibrium Controls are Constant). *For any differential game with unconstrained kinematics described by (1) and a Mayer-type cost functional, the equilibrium strategies of all the agents are constant. In particular, each Attacker's equilibrium trajectory is a straight line (in the Cartesian plane), and the Turret's control is either always clockwise or always counterclockwise.*

Proof. Given that the cost functional is of Mayer-type, the Hamiltonian for the system (1) is

$$\mathcal{H} = \lambda_\beta u_T + \sum_{i=R,P} \lambda_{x_i} \nu \cos \hat{\psi}_i + \lambda_{y_i} \nu \sin \hat{\psi}_i. \quad (14)$$

Let $\hat{\boldsymbol{\lambda}} \equiv [\lambda_{x_R} \quad \lambda_{y_R} \quad \lambda_{x_P} \quad \lambda_{y_P} \quad \lambda_\beta]^\top$ be the adjoint vector in the Cartesian frame. The equilibrium adjoint dynamics are given by [2, Eq. 4.5.3]

$$\dot{\hat{\boldsymbol{\lambda}}} = -\frac{\partial \mathcal{H}}{\partial \hat{\mathbf{z}}} = 0. \quad (15)$$

Without loss of generality, suppose that the Attackers seek to maximize the cost functional while the Turret seeks to minimize it. The equilibrium controls are

$$\cos \hat{\psi}_i^* = \frac{\lambda_{x_i}}{\sqrt{\lambda_{x_i}^2 + \lambda_{y_i}^2}}, \quad \sin \hat{\psi}_i^* = \frac{\lambda_{y_i}}{\sqrt{\lambda_{x_i}^2 + \lambda_{y_i}^2}}, \quad i = R, P \quad (16)$$

$$u_T^* = -\text{sign } \lambda_\beta. \quad (17)$$

Because the equilibrium adjoint dynamics are 0, $\boldsymbol{\lambda}$ is constant, and thus u_T^* and $\hat{\psi}_i^*$ for $i = R, P$ are also constant. Since $\hat{\psi}_i$ are defined relative to the positive x -axis, the Attackers' trajectories are straight lines in the Cartesian plane. \square

Note that if $\lambda_{x_i} = \lambda_{y_i} = 0$ for $i \in \{R, P\}$ then the associated equilibrium heading $\hat{\psi}_i^*$ is not uniquely defined since it would not appear in the Hamiltonian, (14). This generates singular solutions, which will be addressed later.

A. Equilibrium Turret & Runner Strategies

Lemma 2 (Equilibrium Turret Strategy). *In the differential game defined by the kinematics, (2), cost functional, (6), and terminal surface, (7) the Turret's strategy is*

$$u_T^*(t) = k, \quad k \in \{-1, 1\}, \forall t \in [0, t_c]. \quad (18)$$

Proof. The fact that k is a constant is due to Lemma 1. The Turret must minimize the Hamiltonian, (13) – in order to do so, we see that

$$u_T^*(t) = \arg \min_{u_T} \mathcal{H} = \text{sign}(\mu + \sigma_\theta).$$

Again, both μ and σ_θ are constant. The sign function ensures that $k \in \{-1, 1\}$. \square

Lemma 3 (Equilibrium Runner Strategy). *In the differential game defined by the kinematics, (2), cost functional, (6), and terminal surface, (7), the Runner's trajectory is a straight line perpendicular to the Turret's line of sight at the time of termination.*

Proof. The Runner maximizes the Hamiltonian, (13), which occurs when the vector $[\cos \psi_R \quad \sin \psi_R]^\top$ is parallel with the vector $[-\lambda_{r_R} \quad \frac{\mu}{r_R}]^\top$. Therefore,

$$\cos \psi_R^* = \frac{-\lambda_{r_R}}{\sqrt{\lambda_{r_R}^2 + \frac{\mu^2}{r_R^2}}}, \quad \sin \psi_R^* = \frac{\mu}{r_R \sqrt{\lambda_{r_R}^2 + \frac{\mu^2}{r_R^2}}}. \quad (19)$$

At terminal time, $\lambda_{r_R}(t_c) = 0$ from (12), which implies $\cos \psi_{R_c}^* = 0$. Thus A_R 's terminal heading is $\psi_{R_c}^* \in \{\frac{\pi}{2}, -\frac{\pi}{2}\}$, and is perpendicular to T 's line of sight since $\theta_{R_c} = 0$. The fact that A_R 's trajectory is a straight line in the Cartesian coordinate system is due to Lemma 1. \square

It remains to show in which direction (either CCW or CW) both the Turret and Runner should travel. In the present case, wherein $A_R, A_P \notin \mathcal{R}_A$, the biggest benefit for the Attacker team comes when the Runner, A_R , keeps the Turret occupied for as long as possible, thereby giving the Penetrator, A_P , a chance to reach an advantageous position before T starts pursuing A_P in earnest.

Lemma 4. *The sign of the equilibrium Turret and Runner control inputs are such that*

$$\text{sign}(u_T^*) = \text{sign}(\sin \psi_R^*) = \text{sign}(\sin \theta_R). \quad (20)$$

That is, A_R has a component of velocity away from T , and T turns toward A_R .

Proof. There are four possibilities: i) A_R away, T towards, ii) A_R towards, T towards, iii) A_R away, T away, iv) A_R towards, T away. The cost functional (6) is based on the single-Attacker Game of Angle between T and A_P . A_R can only improve the outcome of the 1v1 game if it can cause T to implement a control other than the 1v1 equilibrium strategy (e.g., turn away from A_P rather than towards it). First, consider the Turret's control - if $\text{sign}(u_T) \neq \text{sign}(\sin \theta_R)$ then T is turning away from A_R . In order to neutralize A_R , T must go the long way around the target circle in the worst case. Thus cases iii) and iv) are excluded by inspection. It remains to determine whether

A_R should head i) away from T or ii) towards. At the time A_R would be neutralized in ii), A_R would still be alive in i). The Runner can do nothing to reduce V_{A_P} , but it *can* increase V_{A_P} if it can continue to draw T away from A_P . Therefore, at the time and position of neutralization of A_R in ii) it is never worse (and generally better) for A_R to be alive, which implies A_R must run away from T . \square

Remark. The Turret strategy given by Lemma 2 and Lemma 4 corresponds to the single-Attacker circular target defense strategy from [10] (played against A_R).

Remark. If at any time $\text{sign}(\sin \theta_R) = \text{sign}(\sin \theta_P)$, then the Runner's heading, ψ_R , is inconsequential (i.e., ψ_R^* is not uniquely defined).

The choice of direction for the Turret is to turn towards the two Attackers; by pursuing A_R , the Turret is also pursuing A_P , and thus the Runner can do nothing to help (or hinder) A_P .

B. Equilibrium Penetrator Strategy

The Penetrator seeks to maneuver in such a way to reach an advantageous position by the time the Runner is neutralized. By advantageous, we mean that its terminal position maximizes the Value of the subsequent differential game which ensues once the Runner has been neutralized.

The presence of the Dispersal Surface in the single-Attacker game [8], [10] creates an interesting situation in this two-Attacker variant. When the state of a system lies on a Dispersal Surface, the equilibrium controls of one or more agents is non-unique [2]. In the case of the single-Attacker game, when $\cos \theta = -1$, there is symmetry in the system such that the T could chase A either counterclockwise (CCW) or clockwise (CW) and resulting Value of the Game of Angle would be the same [10]. The consequence of the Dispersal Surface is that the single-Attacker Value function V_{A_P} is not smooth along the surface; thus the single-Attacker adjoint vector, σ , is undefined along the surface. Therefore, A_P 's terminal heading, defined by (22) and (12) as $\psi_{P_c}^* = \tan^{-1} -\sigma_\theta / \sigma_r$, is not well-defined either. There are two cases: (1) $\cos \theta_{P_c} \neq -1$ and σ is well-defined (the regular case), and (2) $\cos \theta_{P_c} = -1$ and σ is undefined (the singular case).

Lemma 5 (Regular Equilibrium Penetrator Strategy). *In the differential game defined by the kinematics, (2), cost functional, (6), and terminal surface, (7) the Penetrator's equilibrium trajectory is a straight line that is aligned with its Game of Angle equilibrium trajectory at terminal time wherever the Game of Angle adjoints σ_r and σ_θ are defined. Moreover, A_P 's control strategy is given by [8], [10]*

$$\sin \psi_P^* = \text{sign}(\sin \theta_{P_c}) \left(\frac{\nu}{r_P} \right). \quad (21)$$

Proof. The Penetrator maximizes the Hamiltonian, (13), which occurs when the vector $[\cos \psi_P \quad \sin \psi_P]^\top$ is parallel with the

vector $[-\lambda_{r_P} \ \sigma_\theta]^\top$:

$$\cos \psi_P^* = \frac{-\lambda_{r_P}}{\sqrt{\lambda_{r_P}^2 + \frac{\sigma_\theta^2}{r_P^2}}}, \quad \sin \psi_P^* = \frac{\sigma_\theta}{r_P \sqrt{\lambda_{r_P}^2 + \frac{\sigma_\theta^2}{r_P^2}}}. \quad (22)$$

At final time, $\lambda_{r_P} = \sigma_r$ (due to (12)) and thus $\tan \psi_P^* = -\sigma_\theta/\sigma_r$. Thus, at final time, A_P 's heading is identical to the equilibrium Attacker heading from the single-Attacker scenario [10]. Furthermore, A_P 's trajectory is a straight line in the Cartesian coordinate frame due to Lemma 1, just as it is in the single-Attacker scenario. Therefore, A_P 's regular state feedback equilibrium control is given by (21). \square

The geometric interpretation of the following Lemma is that the Penetrator's equilibrium trajectory never crosses the $\beta + \pi$ radial. In cases where (21) would cause this, the Runner, instead, takes a shallower angle such that $\cos \theta_{P_c} = -1$.

Lemma 6 (Singular Penetrator Strategy). *In the differential game defined by the kinematics, (2), cost functional, (6), and terminal surface, (7) a family of the Penetrator singular trajectories exist which terminate at $\cos \theta_{P_c} = -1$, with $r_{P_c} > 1$. These trajectories are straight lines with the following state feedback strategy*

$$\sin \psi_P^* = \frac{\chi \nu}{r_P}, \quad (23)$$

where $\chi \in [-1, 1]$ and $\text{sign}(\chi) = \text{sign}(\sin \theta_{P_c})$.

Proof. First, recall that the trajectories are straight lines in the Cartesian coordinate frame due to Lemma 1. The general form of the single-Attacker equilibrium control is given in Lemma 13, in the Appendix:

$$\sin \psi_P^* = \text{sign}(\sigma_\theta) \frac{\nu}{r_P}.$$

However, when $\cos \theta_P = -1$, the term $\text{sign}(\sigma_\theta)$ is undefined because the Value function V_{A_P} is not differentiable on the Dispersal Surface. We replace the quantity $\text{sign}(\sigma_\theta)$ with a variable χ . When $\chi = \pm 1$, the solution exactly corresponds to the limiting case of the regular equilibrium trajectories described in Lemma 5 where $\sin \psi_P^* = \pm \frac{\nu}{r_P}$. If $|\chi| > 1$, the approach angle to the point $(r_P, \cos \theta_P) = (r_{P_c}, -1)$ would be steeper. Backwards integrating from $(r_{P_c}, -1)$ with an angle $|\sin \psi_P| > \frac{\nu}{r_P}$ would push the state of the system into a region that is filled with regular equilibrium trajectories – see Fig. 3. The former trajectories would be suboptimal (nonequilibrium) compared to the latter. Therefore, it must be the case that $\chi \in [-1, 1]$. The sign of χ is governed by the sign of $\sin \theta_{P_c}$ as in the regular trajectory case. Note, this proof method is similar to the method used to solve for the simultaneous capture condition in [26], [27]. \square

The Dispersal Surface in the single-Attacker game (c.f. [10], [11]) favors the Turret. While on the Dispersal Surface ($\theta = \pi$) the Turret may choose to turn either CW or CCW at max turn rate and achieve the same cost in equilibrium. However, for the Attacker to achieve a payoff associated with the equilibrium it must know the Turret's choice at $t = 0$ and choose a corresponding heading (i.e., CW if T chooses CW and CCW otherwise). Without knowing $u_T(0)$, the Attacker is left to

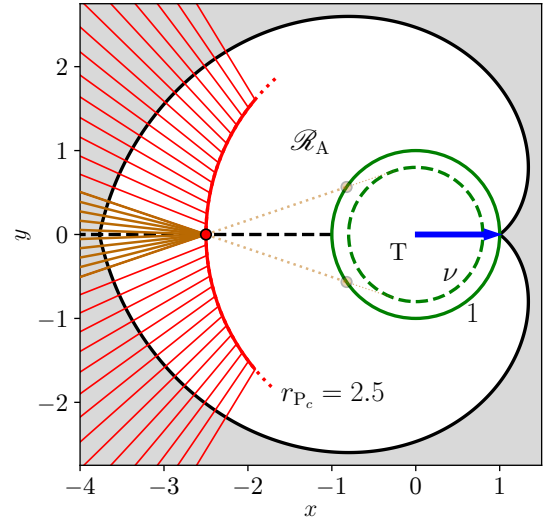


Fig. 3. The Penetrator regular (red) and singular (dark orange) trajectories. The target circle is green; the dashed inner circle is a circle of radius ν ($= 0.8$). Note the extension of each regular A_P trajectory are tangential to the ν circle. The position of the Turret at the time of neutralization of A_R is shown by a blue arrow. A family of trajectories is shown wherein $r_{P_c} = 2.5$. Singular A_P trajectories terminate on the dashed black Dispersal Surface. In the second phase of the scenario, A_P terminates at either dark orange filled circle depending on T's choice of CCW or CW.

guess; a correct guess will yield the equilibrium payoff, and an incorrect guess will result in a small loss in the payoff. In the latter case, the Attacker moves *towards* T at the initial time instant and must immediately switch headings. We observe that the implication for the TRPDG is that the singularity (i.e., $\theta_{P_c} = \pi$) does not benefit the Attacker team.

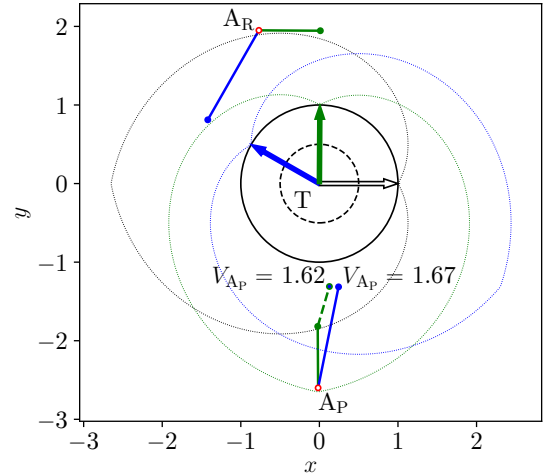


Fig. 4. Comparison of A_R running away (blue) versus towards (green) T. The black arrow represents T's initial position and the dotted lines represent the boundary of \mathcal{R}_A at the time instant associated with its color. In the green case, A_P can make maximal usage of the singularity and aim straight at the target circle. However, the resultant payoff is not as good as in the blue case wherein all three agents implement the prescribed strategies.

Consider the following example, shown in Fig. 4. One may be tempted to believe that the singularity could be *helpful* to the Attacker team in the sense that, under the prescribed Penetrator strategy, A_P may run directly towards the closest

point on the target circle (thereby reducing r_P as quickly as possible). In this example, A_R , contrary to Lemma 4 runs towards T who turns CCW (shown in green). A_P is placed directly on the line $\theta_{R_c} = \pi$; this is the most “extreme” example of A_P taking a singular path (i.e., being able to set $\psi_P = 0$). The blue trajectory corresponds to A_R running away from T and A_P taking the heading prescribed in (21). For the green case, $\theta_{P_c} = \pi$ but neutralization of A_R happens much sooner, whereas in the blue case $\theta_{P_c} < \pi$ but neutralization of A_R is later. The green Penetrator trajectory is continued with a dashed line for the CCW case up until T reaches the blue position. In this case, if T goes CCW the entire time, then clearly it is better for A_P to play according to the associated 1v1 strategy of aiming at the tangent to the circle of radius ν . Hence, the blue trajectories (which follow the prescribed strategies) yield the best Value for the Attackers.

C. Full solution

Figure 5 shows the state trajectory in the Cartesian coordinate frame for a regular trajectory (with $\cos \theta_{P_c} \neq -1$) and for a singular trajectory (with $\cos \theta_{P_c} = -1$). The Runner, A_R , has a trajectory which is perpendicular to the Turret’s line of sight at the time of termination. In the regular case, the Penetrator, A_P , has a trajectory which is aimed at the tangent of a circle of radius ν ; once A_R is neutralized, A_P would continue along this course all the way to the target circle. In the singular case, the Penetrator prefers not to cross the $\cos \theta_P = -1$ radial at $t = t_c$ and therefore has taken a shallower angle to end up at $\cos \theta_{P_c} = -1$. From here, the Penetrator takes either the upper or lower trajectory depending on T’s choice of rotation after neutralizing A_R (CW or CCW, respectively).

Although it wasn’t explicitly stated in the problem formulation, we require that $\cos \theta_P \neq 0$ for all $t \in [0, t_c]$ because, otherwise, the Penetrator would have been neutralized while T was *en route* to neutralize the Runner. The limiting case occurs when $\text{sign}(\sin \theta_P) = \text{sign}(\sin \theta_R)$ and $\cos \theta_P \rightarrow 0$ precisely at the moment of neutralization of A_R .

In order for A_P to penetrate the target, it must reach $\mathcal{R}_{A_c} \equiv \mathcal{R}_A(\mathbf{z}(t_c))$, i.e., the one-on-one Attacker win region at terminal time. The limiting case occurs when $A_{P_c} \in \partial \mathcal{R}_{A_c}$ where $\partial \mathcal{R}_{A_c}$ is the boundary of the one-on-one Attacker win region at terminal time. That is, the Penetrator is just barely able to satisfy the necessary condition to ‘win’ (i.e., reach the target) in the second phase of the engagement. Note that $\partial \mathcal{R}_{A_c}$ is the zero-level set of the cost functional, V_{A_P} , and thus the equilibrium Penetrator trajectories terminating at a point on $\partial \mathcal{R}_{A_c}$ are normal to the surface. The other limiting case is when A_P reaches the target exactly when A_R is neutralized.

Define \mathcal{R}_{2A} as the set of states in which A_P can be guaranteed to ‘win’, i.e., the set of states in which $A_P \in \mathcal{R}_A$ within t_c time while avoiding premature termination. One boundary of $\partial \mathcal{R}_{2A}$ can be constructed geometrically by setting A_P on $\partial \mathcal{R}_{A_c}$ and backwards integrating the equilibrium Penetrator strategy ((21) for $\cos \theta_{P_c} \neq -1$, and (23) for $\cos \theta_{P_c} = -1$). The other boundary is obtained by setting $r_P = 1$ and backwards integrating. Care must be taken to

eliminate terminal A_P positions which result in A_P paths which start and end inside the sector swept by the T’s motion (which would result in premature termination.) Figure 6 shows a slice of \mathcal{R}_{2A} for a particular initial Turret position (β) and A_R position ((r_R, θ_R)).

It’s clear from Fig. 6 and Eqs. (21) and (23) that the solution depends on β_c (from which θ_{P_c} is measured), or equivalently, the terminal time, t_c . From Lemmas 2 and 3, along with Lemma 4, we know that A_R has a component of velocity directed away from T and terminates perpendicular to T’s line of sight under optimal play, while T moves in the direction of A_R at its maximum turn rate. Thus T must cover an angular sector at least $\text{mod}(|\theta_R|, 2\pi)$. For the Turret, angle traveled and time are equivalent since the Turret’s turn rate and the target circle radius are both 1. Let $\gamma \geq 0$ be the amount of additional angle the Turret must cover to neutralize the Runner. Then $t_T = \text{mod}(|\theta_R|, 2\pi) + \gamma$ is time of arrival of the Turret to the candidate terminal position. The Runner’s trajectory to the candidate terminal configuration covers an angular sector γ and is perpendicular to T’s line of sight in the terminal configuration. See Fig. 7 for a diagram depicting the geometry. Thus $t_A = \frac{1}{\nu} r_R \sin \gamma$ is the time of arrival of the Runner to the candidate terminal position. In the limiting case, the terminal

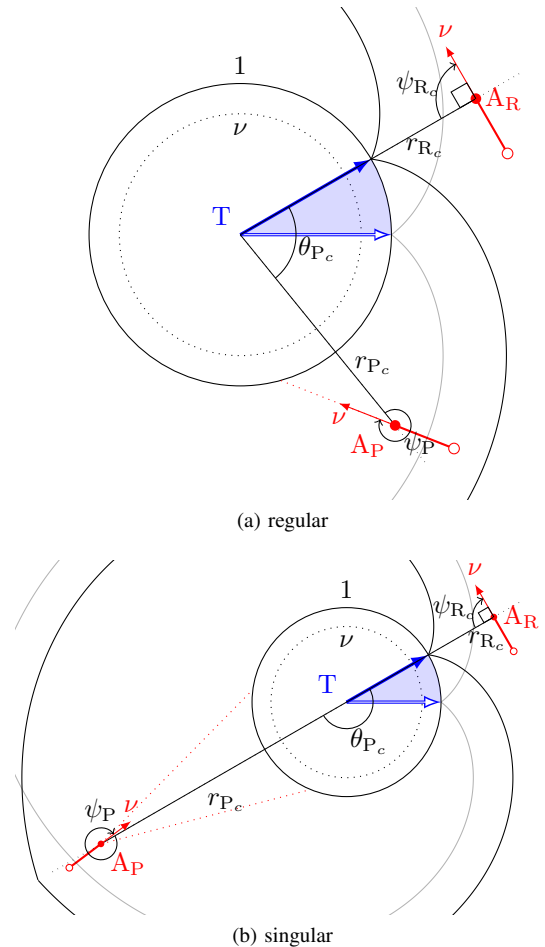


Fig. 5. Representative solutions for the (a) regular and (b) singular cases. Initial Attacker and Turret positions are denoted by open circles and an arrow, respectively; terminal positions are filled. The boundary of \mathcal{R}_A is shown at $t = 0$ (grey) and at $t = t_c$ (black).

Runner distance is $r_{R_{\min}} = 1$, which gives an upper bound for γ :

$$\gamma_{\max} = \cos^{-1}\left(\frac{1}{r_R}\right).$$

Now, define the time difference of arrival to the terminal configuration as

$$\begin{aligned} \tau(\gamma) &\equiv t_T(\gamma) - t_A(\gamma) \\ &= |\theta_R| + \gamma - \frac{1}{\nu} r_R \sin \gamma, \end{aligned} \quad (24)$$

with $\gamma \in [0, \cos^{-1}(1/r_R)]$. Clearly it would be suboptimal for the Runner to reach a point, stop, and wait for the Turret to reach that point (i.e., $\tau > 0$); similarly, if the Turret arrives before the Runner (i.e., $\tau < 0$) the Turret would have had to pass the Runner *en route*. Thus, for equilibrium, it must be the case that both agents arrive in the terminal configuration simultaneously, i.e., $\tau^* = 0$.

Lemma 7. *The function, $\tau(\gamma)$, (24), which represents the time difference of arrival of the Runner and Turret to a candidate terminal configuration, has a unique zero, γ^* , on the interval $[0, \cos^{-1}(1/r_R)]$.*

Proof. First, (24) is a continuous function of γ since γ and $\sin \gamma$ are both continuous. For the lower bound of τ , we have $\tau(0) = \text{mod}(|\theta_R|, 2\pi)$, and thus $\tau(0) > 0$. In other words the

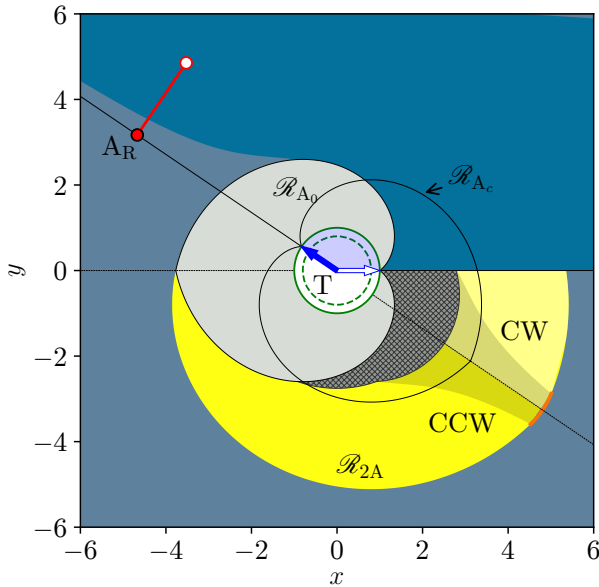


Fig. 6. A partitioning of the state space for particular β , r_R , and θ_R . The T and A_R trajectories start at the open circles and end at the closed circles. The *Game of Kind* surface θ_{GOK} is drawn at $t = 0$ and at $t = t_c$. Note we do not consider A_P positions beginning within \mathcal{R}_{A_0} , marked by light grey, nor positions in which A_P penetrates the target before t_c , marked by hatched grey. The yellow region represents \mathcal{R}_{2A} , the set of A_P initial conditions which in which it can be guaranteed to successfully penetrate the target. In the light shaded portion, A_P 's motion has a clockwise component, otherwise it has a counter-clockwise component. The dark shaded portion is filled with singular trajectories which terminate on $\cos \theta_{P_c} = -1$. There is a segment of $\partial \mathcal{R}_{2A}$ which is a circular arc, marked by orange, which is the locus of extremal A_P singular initial conditions. Premature termination would occur for any A_P positions beginning in the bright blue region, and the faded blue region represents positions in which \mathcal{R}_{A_c} cannot be reached; T is able to neutralize both Attackers in either case.

Runner arrives first – in fact, it travels zero distance, whereas the Turret covers $\text{mod}(|\theta_R|, 2\pi)$ angular distance. For the upper bound, we will show that $\tau(\gamma_{\max}) < 0$ by contradiction. Suppose that $\tau(\gamma_{\max}) > 0$, that is, the Runner arrives to the candidate terminal configuration before the Turret. The upper bound, γ_{\max} is derived from the limiting case where $r_{R_c} \rightarrow 1$. This would mean the Runner was able to reach the target circle before the Turret could align with it which contradicts the assumption that $A_R \notin \mathcal{R}_A$ (which is embedded in the assumption that $\mathbf{z} \in \Omega$). Therefore, from the Intermediate Value Theorem, the function $\tau(\gamma)$ crosses zero on the interval $[0, \cos^{-1}(1/r_R)]$.

Also, $\partial \tau / \partial \gamma = 1 - r_R / \nu \cos \gamma$ which is strictly negative on the interval $[0, \cos^{-1}(1/r_R)]$ since $r_R / \nu > 1$ and $\cos \gamma > 0$ on the interval. Thus $\tau(\gamma)$ is monotonic on the interval, which implies that the zero crossing is unique. \square

Because of the uniqueness of γ^* in which $\tau(\gamma^*) = 0$ many standard root-finding methods are suitable for computing it. The terminal time is simply

$$t_c = \text{mod}(|\theta_R|, 2\pi) + \gamma^*. \quad (25)$$

With the value of t_c computed, we obtain $\beta_c = \beta + t_c \text{sign}(\sin \theta_R)$. From Fig. 6 we see that the effect of $\text{sign}(\sin \theta_{P_c})$ in (21) and (23) is that the Runner's motion (at least in \mathcal{R}_A) has a component of velocity towards the $\beta_c + \pi$ radial. The interpretation is that the Runner seeks to end up *behind* the Turret at terminal time, which is an advantageous position for the *Game of Angle*. Thus, under equilibrium play by all the agents, the terminal state is

$$\mathbf{z}_c = \begin{bmatrix} r_{R_c} \\ \theta_{R_c} \\ r_{P_c} \\ \theta_{P_c} \\ \beta_c \end{bmatrix} = \begin{bmatrix} r_R \cos(t_c - \text{mod}(|\theta_R|, 2\pi)) \\ 0 \\ \sqrt{\left(\frac{\nu^2 \chi t_c}{r_P}\right)^2 + \left(r_P - \nu t_c \sqrt{1 - \frac{\chi^2 \nu^2}{r_P^2}}\right)^2} \\ \theta_P - \text{sign}(\sin \theta_R) t_c + \sin^{-1}\left(\frac{\chi \nu^2 t_c}{r_P r_{P_c}}\right) \\ \beta + \text{sign}(\sin \theta_R) t_c \end{bmatrix}, \quad (26)$$

where $\chi \in \{-1, 1\}$ for regular trajectories, $\chi \in [-1, 1]$ for singular trajectories, and

$$\text{sign } \chi = \text{sign}(\sin \theta_{P_c}) = \text{sign } \xi, \quad (27)$$

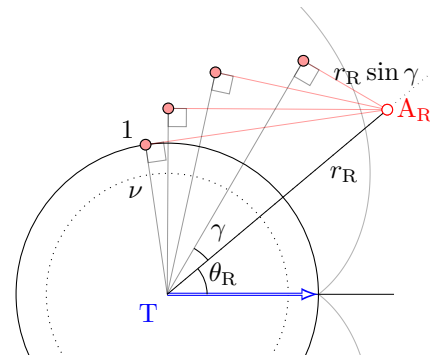


Fig. 7. Relevant geometry for the determination of terminal time t_c . Open circles represent initial positions and the closed red circles indicate candidate terminal configurations for A_R .

where $\xi \in [-\pi, \pi]$ is A_P 's angle-to-go to the $\beta_c + \pi$ radial,

$$\xi = -\text{mod}(\theta_P - \text{sign}(\sin \theta_R) t_c, 2\pi) + \pi. \quad (28)$$

The trajectory is singular if A_P 's regular strategy, (21), would cause it cross the $\beta_c + \pi$ radial, which occurs if

$$\sin^{-1} \left(\frac{\nu^2 t_c}{r_P \sqrt{r_P^2 + \nu^2 t_c^2 - 2r_P \nu t_c \sqrt{1 - \frac{\nu^2}{r_P^2}}}} \right) > |\xi|. \quad (29)$$

Note the LHS of the above expression is the angular sector swept (w.r.t. the origin) by A_P 's regular strategy in t_c time. If the trajectory is singular, then, by definition $\cos \theta_{P_c} = -1$. The Law of Sines gives the following relationships:

$$\frac{r_{P_c}}{\sin \psi_P} = \frac{\nu t_c}{\sin \xi} = \frac{r_P}{\sin(\pi - |\psi_P| - |\xi|)}.$$

The singular A_P heading is

$$\psi_P = \text{sign}(\xi) \left(\sin^{-1} \left(\frac{r_P \sin |\xi|}{\nu t_c} \right) - |\xi| \right), \quad (30)$$

and the singular terminal A_P distance is

$$r_{P_c} = \frac{\nu t_c \sin \psi_P}{\sin \xi}. \quad (31)$$

Finally, the Value function is

$$V(\mathbf{z}) = |\theta_{P_c}| - \theta_{GoK}(r_{P_c}), \quad (32)$$

where (r_{P_c}, θ_{P_c}) is given by (26) and θ_{GoK} is defined in (48). Note that, in general, the Attacker win regions, \mathcal{R}_A and \mathcal{R}_{2A} , are larger in size for larger ν .

The Attackers simply aim at their respective terminal point from (26), and the Turret rotates towards the Runner. Of course, one or more agents could (to their detriment) deviate from the strategy which would necessitate recomputing the solution in practice. For discrete time systems, for example, it is recommended for the agent implementing its equilibrium strategy to recompute the solution at each time step.

Figure 8 contains an example in which the Attackers both lose when operating individually, but one is able to win when the Attackers cooperate and behave according to the solution of the TRPDG.

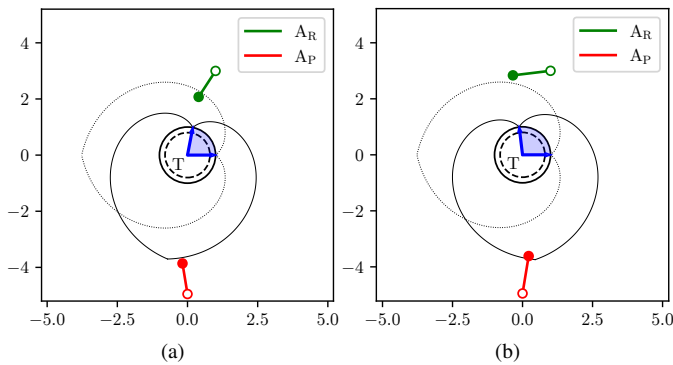


Fig. 8. Attackers implement single-Attacker strategy, ignoring the presence of the other Attacker (a); neither Attacker wins. Attackers cooperate, implementing the TRP solution (b); A_P wins as a result.

IV. TRPDG WITH EARLY PENETRATION

In this section we analyze the case in which the Penetrator can reach the target circle prior to the capture of the Runner. Such is the case, e.g., in the hatched region of Fig. 6.

We assume the Turret prefers to pursue (and eventually neutralize) the Runner rather than attempt to reduce the Penetrator's angular separation at the time of penetration. If the Turret were to attempt to minimize $|\theta_P|$ it may be the case A_R could reach a more advantageous position – perhaps even inside \mathcal{R}_A . We therefore fix the Turret's strategy to $u_T = \text{sign}(\sin \theta_R)$ as it is in the previous section. Additionally, the Runner strategy from the previous section is utilized in the following analysis.

With the Turret and Runner strategies fixed, the EP case becomes an optimal control problem for the Penetrator. Let t_f be the time instant at when the Penetrator actually penetrates the target circle. Then the cost functional is the same as in (4) and is restated here with some additional notation.

$$J^E = \Phi^E(\mathbf{z}(t), t_f) = |\theta_P(t_f)|, \quad (33)$$

where $0 \leq t_f \leq t_c$ and the superscript E denotes Early Penetrator (EP). The Penetrator seeks to maximize its angular separation *at the time of penetration*. For the sake of clarity, let reaching the target circle and penetrating the target be defined as $r_P = 1$ and $r_P < 1$, respectively. The Value of the EP optimal control problem, if it exists, is defined as

$$V^E(\mathbf{z}_0) \equiv \max_{\psi_P(\cdot)} J^E. \quad (34)$$

An important distinction must be made at this point as to whether or not the Penetrator has anything to gain (according to (33)) by delaying penetration. If, for example, $|\dot{\theta}_P| < 0$ when the Penetrator has reached the target circle then it only stands to reduce its payoff by delaying penetration and thereby chooses to end the game by penetrating the target immediately upon arrival. However, delaying penetration is advantageous, for example, when the Turret's pursuit of the Runner is drawing its aim further away from the Penetrator at the time of arrival at the target (i.e., $|\dot{\theta}_P| > 0$).

A. Regular Trajectories Ending in Immediate Penetration

For regular trajectories ending in immediate penetration it is necessary that 1) $\text{sign}(\sin \theta_P) = \text{sign}(\sin \theta_R)$ or 2) $\text{sign}(\sin \theta_R) \sin \theta_P < \text{sign}(\sin \theta_R)(t_c - \pi)$. In the former case, the two Attackers are on the same side w.r.t. the Turret's look angle. Once the Penetrator reaches the target circle (i.e., $r_P = 1$) it can only be the case that $|\dot{\theta}_P| < 0$ because $\nu < 1$ and thus T has an angular velocity advantage. Case 2) corresponds to $\text{sign}(\sin \theta_{P_c}) = \text{sign}(\sin \theta_R)$, and thus the direction of A_P 's motion is the same as A_R and T's (c.f. III-B). Satisfaction of this condition, alone, is not sufficient. For example, it may be possible for A_P to achieve $\cos \theta_{P_f} = -1$, thereby the trajectory would be singular (to be discussed in the following subsections). The regular optimal penetrator strategy is given by (21) defined over $t \in [0, t_f]$.

B. Delayed Penetration

When the Turret is turning away from the Penetrator, it is advantageous for the Penetrator to delay penetration until the Runner's neutralization at t_c ; thus $t_f = t_c$. We begin by augmenting the problem definition by including the following path constraint

$$m(\mathbf{z}) = r_P - 1 \geq 0, \quad \forall t \in [0, t_c], \quad (35)$$

which requires that A_P remain on or outside the target circle until the moment of A_R 's neutralization by T. When the constraint is active, the system may remain constrained if $\dot{r}_P = 0$. From (2) we have

$$\dot{r}_P = -\nu \cos \psi_P,$$

and thus the system will remain constrained if $\psi_P = \pm \frac{\pi}{2}$.

Note that the terminal manifold, the zero-level set of ϕ (defined in (7)), is only defined over $r_{P_c} \geq 1$. From (12) the terminal adjoint values depend on $\frac{\partial \phi}{\partial \mathbf{z}_c}$. Thus, when $r_{P_c} = 1$, the quantity $\frac{\partial \phi}{\partial r_{P_c}}$ is undefined (since the state is on edge of the bounded plane $\phi = 0$). Consequently, from (22), it is clear that the optimal Penetrator heading at terminal time, $\psi_{P_c}^*$, is undefined. This is another singularity which is similar to the $\cos \theta_{P_c} = -1$ singularity analyzed in Section III-B.

The following subsections treat the $r_{P_c} = 1$ singularity and the constrained trajectories. We refer to the $r_{P_c} = 1$ and $\cos \theta_{P_c} = -1$ singularities as the *distance singularity* and *angle singularity*, respectively.

1) *Distance Singularity*: The following lemma provides bounds on the value of the terminal Penetrator heading for this case.

Lemma 8. *For EP, if $r_{P_c} = 1$ and $\cos \theta_{P_c} \neq -1$, the terminal Penetrator heading is bounded according to*

$$\text{sign}(\sin \theta_{P_c}) \sin^{-1} \nu \leq \text{sign}(\sin \theta_{P_c}) \psi_{P_c}^* \leq \text{sign}(\sin \theta_{P_c}) \frac{\pi}{2}. \quad (36)$$

Proof. The inclusion of $\text{sign}(\sin \theta_{P_c})$ is necessary to account for the fact that A_P seeks to aim towards the $\beta_c + \pi$ radial, which maximizes its payoff (c.f., Section III-B). The upper bound of (36) is due to the path constraint, $r_P \geq 1$. A larger heading angle would yield $\dot{r}_P > 0$, which implies that A_P had arrived at the target circle from the inside, which clearly violates the constraint. The lower bound corresponds to the regular/unconstrained Penetrator control, (21). A smaller heading angle would push the state of the system into a region where regular/unconstrained trajectories exist. They, by definition have $r_{P_c} > 1$ and $|\theta_{P_c}|$ necessarily smaller. Thus coming in to $r_{P_c} = 1$ with this heading would have been suboptimal for the Penetrator. \square

For any $|\psi_{P_c}| \in [\sin^{-1} \nu, \frac{\pi}{2})$, we have $\dot{r}_2 < 0$ and thus the system immediately leaves the constraint in backwards time. The following Lemma gives the optimal Penetrator heading for this case.

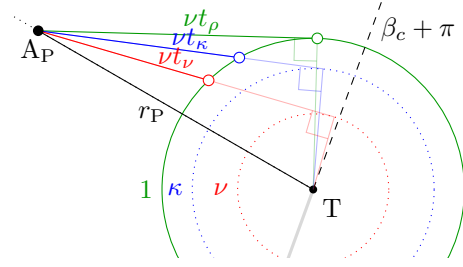


Fig. 9. An illustration of three time instants of interest: t_ν , the time required for A_P to reach the target circle whilst aiming at the tangent to the ν circle, t_κ , the time to reach the target circle whilst aiming at the tangent to the κ circle, and t_ρ , the time to reach the target circle tangentially.

Lemma 9. *For EP, if the constraint m is active only at terminal time, that is, if $r_P > 1$ for $t \in [0, t_c)$ and $r_{P_c} = 1$, and $\theta_{P_c} \neq \pi$ the optimal Penetrator heading is*

$$\sin \psi_P^* = \text{sign}(\sin \theta_{P_c}) \left(\frac{\kappa}{r_P} \right), \quad (37)$$

where

$$\kappa = +\sqrt{\frac{4r_P^2 - (\nu^2 t_c^2 - r_P^2 - 1)^2}{4\nu^2 t_c^2}}, \quad (38)$$

and $\nu < \kappa < 1$.

Proof. Because the trajectory is unconstrained (except for at the moment of termination), Lemma 1 applies, which means A_P 's trajectory is a straight line in the Cartesian plane. The premise of this Lemma is that A_P ends on the target circle, thus we need only determine the line segment joining A_P 's position to a point on the target circle which is of length νt_c , which is the distance A_P can cover in the time it takes T to neutralize A_R . Consider a circle of radius κ , $\nu < \kappa < 1$, centered at the origin. The distance from A_P to a tangent point on the κ circle is $\sqrt{r_P^2 - \kappa^2}$ (see Fig. 9). Since $\kappa < 1$, the line segment joining A_P to the tangent point passes through the target circle. The distance from this intersection to the tangent point on the κ circle is $\sqrt{1 - \kappa^2}$. Thus the time it takes for A_P to reach the target circle while aiming at a tangent point on the κ circle is

$$t_\kappa = \frac{1}{\nu} \left(\sqrt{r_P^2 - \kappa^2} - \sqrt{1 - \kappa^2} \right). \quad (39)$$

Eq. (38) is obtained by setting the above expression equal to t_c and solving for κ . Finally, (37) is obtained from the right-triangle geometry, since A_P 's aim point is tangent to the κ circle, and, once again, $\text{sign}(\sin \theta_{P_c})$ appears for reasons described in Lemma 5. \square

2) *Constrained Trajectories*: The following Lemma provides the optimal Penetrator heading for the case where the trajectory is constrained (or partly constrained).

Lemma 10. *For EP, if the constraint m activates at a time t_ρ , where $0 \leq t_\rho \leq t_c$ the optimal Penetrator heading is*

$$\sin \psi_P^* = \begin{cases} \text{sign}(\sin \theta_{P_c}) \left(\frac{1}{r_P} \right) & 0 \leq t < t_\rho, r_P > 1, \\ \text{sign}(\sin \theta_{P_c}) & t_\rho \leq t \leq t_c, r_P = 1, \end{cases} \quad (40)$$

where

$$t_\rho = \frac{1}{\nu} \sqrt{r_P^2 - 1}. \quad (41)$$

Proof. In this case, the constraint m is activated partway through the trajectory. The trajectory may be considered as two parts: an unconstrained arc, \mathcal{U} (wherein $r_P > 1$), and a constrained arc, \mathcal{C} ($r_P = 1$). In the transition from \mathcal{U} to \mathcal{C} , it is necessary that there exist controls ψ_P and/or u_T that keep the system on the constraint (i.e., maintain $m = 0$). This is referred to as the tangency condition [25]. Here, the Penetrator heading, ψ_P , appears in the expression $\dot{m} = \dot{r}_P = -\nu \cos \psi_P$, and thus the system may remain constrained if the Penetrator applies a heading s.t. $\dot{m} = 0$ which is $\psi_P = \pm \frac{\pi}{2}$. Over the \mathcal{U} arc, the results of Lemma 1 apply, which states the Penetrator trajectory is a straight line in the Cartesian plane. Thus the Penetrator must reach the target circle tangentially, in a straight line, and proceed thereafter by traveling along its perimeter until terminal time. The time at which A_P reaches the target circle tangentially, (41), is obtained from the relevant right-triangle geometry (see Fig. 9). Eq. 40 is then synthesized from the controls associated with the \mathcal{U} and \mathcal{C} arcs. The inclusion of $\text{sign}(\sin \theta_{P_c})$ is necessary for reasons discussed in Lemma 5. \square

3) *Case Determination:* From Fig. 9 and the delayed penetration control policies in Lemmas 9 and 10, the conditions which determine the type of trajectory based on the system's current state may be established. Let t_κ and t_ρ be defined as in (39) and (41), respectively. Also, t_ν (as depicted in Fig. 9) can be derived:

$$t_\nu = \frac{1}{\nu} \left(\sqrt{r_P^2 - \nu^2} - \sqrt{1 - \nu^2} \right). \quad (42)$$

If $t_\nu > t_c$, then A_P , employing the regular optimal strategy, (21), could not have reached the target circle by the time of A_R 's neutralization (then the optimal penetrator control is governed by Lemma 5). Else if $t_\nu \leq t_c < t_\tau$, there exists a straight line trajectory terminating on the target circle of length νt_c (Section IV-B1, Lemma 9). Otherwise, $t_c \geq t_\tau$ and A_P can aim at a tangent point to the target circle, reach the target circle, and apply the constrained control until $t = t_c$ (Section IV-B2, Lemma 10).

C. Max Payoff Possible

In this subsection we address the case in which the upper limit of the cost/payoff functional, (33), is realizable (i.e., $J = \pi$). Recall from Section III-B the singularity which arises when $\cos \theta_{P_c} = -1$ – that is, the Turret is looking directly away from the Penetrator at terminal time. There, the terminal Penetrator heading $\psi_{P_c}^*$ was undefined according to the first-order necessary conditions for equilibrium. This singularity also comes into play for the two early penetrator cases discussed so far.

Consider the case where $(r_{P_c}, \cos \theta_{P_c}) = (1, -1)$ which is the corner of the bounded plane $\phi = 0$ and the intersection of the distance and angle singularities. In Section III-B, the angle singularity gave rise to a symmetric cone of incoming trajectories bounded by $\psi_{P_c}^* \in \left[-\sin^{-1} \left(\frac{\nu}{r_{P_c}} \right), \sin^{-1} \left(\frac{\nu}{r_{P_c}} \right) \right]$. In

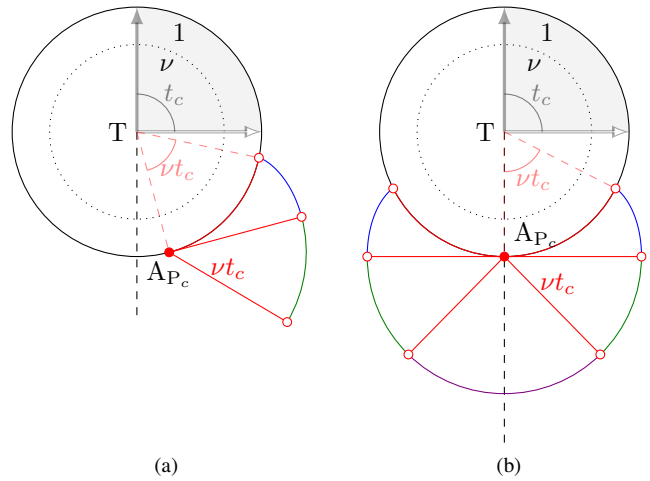


Fig. 10. Delayed penetration case (a) away from the angle singularity and (b) at the angle singularity. The curve shows the locus of initial A_P positions which terminate at the point shown. Blue sections are involutes, green sections are circular sectors corresponding to the distance singularity, and the purple section in (b) is a circular sector corresponding to the angle singularity.

Section IV-B1, the distance singularity gave rise to a cone of incoming trajectories bounded by $\sin^{-1}(\nu)$ and $\frac{\pi}{2}$. The combination of the two singularities results in a cone of incoming trajectories bounded by,

$$-\frac{\pi}{2} \leq \psi_{P_c}^* \leq \frac{\pi}{2}. \quad (43)$$

The locus of initial A_P positions thus forms a semi-circle of radius νt_c centered on $(r_{P_c}, \cos \theta_{P_c}) = (1, -1)$. Concerning constrained trajectories with $\psi_{P_c} = \pm \pi$, the optimal trajectories emanate in both directions in backwards time. Figure 10b shows the locus of initial Penetrator positions which terminate on the corner point exactly at $t_f = t_c$.

Remark. For initial A_P positions which lie *inside* the locus shown in Fig.10b the optimal Penetrator heading ψ_P^* is non-unique.

The non-uniqueness of A_P 's control in this region is due to the fact that the cost functional, (33), is upper-bounded by π . Termination at the corner point ($(r_P, \cos \theta_P) = (1, -1)$) achieves the upper-bound for A_P 's payoff; thus any trajectory which reaches the corner point within t_c time is an optimal trajectory for A_P .

D. Full Solution

To summarize the solution of the Early Penetrator optimal control problem within the TRPDG, we construct the regions for which each particular Penetrator control is optimal. The green region in Fig. 11 corresponds to the immediate penetration case (Section IV-A). For initial A_P positions in the yellow region, the Penetrator aims clockwise and penetrates exactly at the moment A_R is neutralized at $t = t_c$ (see Section IV-B). Lastly, the red region represents all the positions from which A_P can reach $(r_P, \cos \theta_P) = (1, -1)$. The ‘‘Max Value’’ region arises from the fact that A_P may penetrate the target at any time $t_f \in [0, t_c]$, and thus we must consider the distance and angle singularities as shown in Fig. 10b for all possible t_f . The

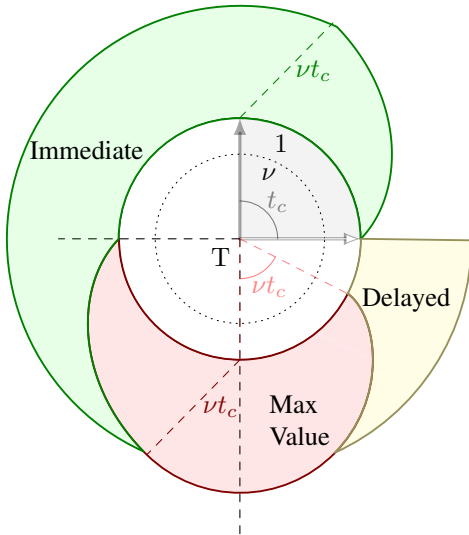


Fig. 11. Solution of the Early Penetrator optimal control problem for $t_c = \frac{\pi}{2}$.

red region in Fig. 11 is the union of all such regions. Inside the red region, the Penetrator may be able to reach $(1, -1)$ for a continuum of different t_f .

V. ROLE SELECTION

In the previous sections we considered the roles of A_R and A_P to be fixed, *a priori*, to Runner and Penetrator, respectively. The Turret adhered to this convention by blindly pursuing the Runner, regardless of the position of the Penetrator. Moreover, we restricted the formulation such that the roles could not switch. We now consider the more likely scenario in which the roles of the Attackers are not specified; thus the Turret gets to choose which Attacker to pursue (continuously throughout the game). Let the Attackers be specified generally as A_1 and A_2 .

In order to specify the equilibrium “status” of the TRPDG policies in the context of this more general version of the problem, we introduce the following definitions.

Definition 1. The Global Stackelberg Equilibrium (GSE) [28], [29] is an equilibrium over open-loop strategies; the *leader* selects a control trajectory (defined over $t = 0$ to the end of the game) from a specified class of behaviors and announces the strategy to the *follower*. The equilibrium arises when the *follower* plays its best response to the announced strategy, and the *leader*, knowing this, selects its best control trajectory.

Definition 2. A pair of strategies forms a subgame perfect equilibrium (or *time consistent* equilibrium) if the strategies are in equilibrium for every subgame of the game’s play-out [30]. That is, in order for the strategy pair to be subgame perfect, it must never become advantageous for one or other agent to switch strategies at any point along the game’s trajectory.

Definition 3. The State-Feedback Nash Equilibrium (SFNE) [29], [31] is an equilibrium over closed-loop (state-

feedback) strategies corresponding to the saddle point of the cost functional (in the case of zero-sum differential games).

When a strategy pair constituting the GSE yields a trajectory which is subgame perfect, the strategy pair is also the SFNE for all of the points along the trajectory.

For the context of the TRPDG with role selection, let us consider a new action space for the agents. The Turret must only decide to turn CCW or CW at $t = 0$, which effectively determines which Attacker will be the Penetrator and which Attacker will be the Runner. From there, all 3 agents proceed according to their TRPDG equilibrium controls associated with this assignment (according to Section III). Let the Value associated with the two assignments be defined

$$V_{1,2}(A_1, A_2) \equiv V \left([r_1 \ \theta_1 \ r_2 \ \theta_2 \ \beta]^\top \right), \quad (44)$$

$$V_{2,1}(A_2, A_1) \equiv V \left([r_2 \ \theta_2 \ r_1 \ \theta_1 \ \beta]^\top \right), \quad (45)$$

where V is defined in (8). Thus, e.g., $V_{2,1}$ is the Value of the TRPDG with A_2 assigned to Runner and A_1 assigned to Penetrator.

Lemma 11. *The TRPDG strategies given in Section III corresponding to $\min(V_{1,2}, V_{2,1})$ constitute a GSE with the Turret as the leader and Attackers as the follower. The associated Value of the Stackelberg Game is $V_S = \min(V_{1,2}, V_{2,1})$, where the subscript S denotes “Stackelberg”.*

Proof. By construction, the strategies satisfy the first-order necessary conditions for equilibrium. Now it remains to show that the Value, V_S , is given by the minimum of the TRPDG Value associated with each assignment. The Value of the TRPDG, (32), is mathematically premised on the fact that the only way to terminate the game is by neutralizing the Runner (i.e., the terminal surface is $\theta_R = 0$, see (7)). Thus the formulation ignores the possibility of neutralization of the Penetrator (i.e., by driving $\cos \theta_P \rightarrow 1$). The TRPDG Value functions (without role selection) satisfy the saddle-point equilibrium property

$$J(u_T^*, \psi_i, \psi_j) \leq V_{i,j} \leq J(u_T, \psi_i^*, \psi_j^*), \quad i, j \in \{1, 2\}. \quad (46)$$

So, in the general scenario in which T can choose which Attacker to neutralize, only T’s side (the left side) of the saddle-point property holds – that is, T can do no worse than the TRPDG Value associated with each direction. Therefore, T is free to choose the smaller of the two. The Attackers’ best response is to respond accordingly, assigning the Runner and Penetrator roles as dictated by T’s choice. Thus T pursues A_1 if $V_{1,2} < V_{2,1}$, otherwise, it is better to pursue A_2 first. \square

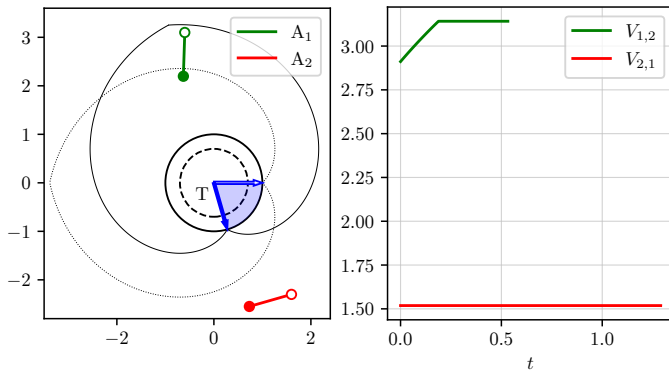
It appears that the GSE is also the SFNE everywhere in the state space. However, we leave a rigorous proof of such for future work.

VI. SIMULATIONS

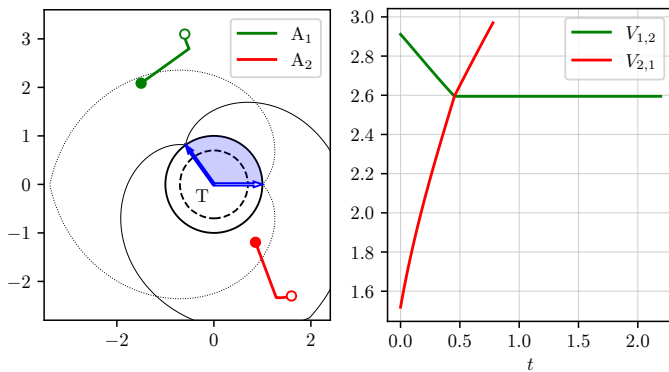
In this section, we present some simulation results wherein the prescribed strategies are implemented in a discrete-time fashion. In particular, the agents’ control signal is held constant over a fixed time interval (which we denote as Δt) and all

agents' controls are updated synchronously as a function of the current state only. Neither agent has access to its opponents current control action (unlike in the Stackelberg version of the game).

The assignment of roles for the Attackers is not specified. Instead, the "equilibrium" action involves comparing $V_{1,2}$ and $V_{2,1}$ (at the current time) and implementing the TRPDG controls associated with the lesser Value (as described in the previous section). The Value of the "wrong" sequence (i.e., $\max(V_{1,2}, V_{2,1})$) is of the utmost importance in demonstrating whether or not a GSE trajectory is subgame perfect (and thus also SFNE). Thus, in Fig. 12, both values, $V_{1,2}$ and $V_{2,1}$, are computed along the entire trajectory.



(a) Equilibrium – all agents implement controls associated with $\min(V_{1,2}, V_{2,1})$.



(b) Attackers implement equilibrium strategy, and the Turret chooses to pursue A_1 first.

Fig. 12. Simulation results; $\nu = 0.7$, $\Delta t = 1e - 3$. Once the Attacker designated as Runner crosses into \mathcal{R}_A , the associated Value of the TRPDG does not exist, which is the reason for the reason for, e.g., $V_{1,2}$ stopping early in (a).

As shown in Fig. 12a, when all 3 agents implement the GSE strategy (corresponding to A_2 being Runner and A_1 being Penetrator) the Value $V_{2,1}$ is constant and remains the smaller of the two Values throughout the ployout of the game. This trajectory is subgame perfect, and thus the GSE and SFNE are equivalent for all points along this trajectory.

Figure 12b demonstrates what happens when T deviates by pursuing A_1 first. Without knowing T's current or future control actions, the Attackers proceed with implementing the equilibrium strategy (treating A_2 as the Runner). Around $t = 0.5$, the TRPDG Values of the two assignments cross, and immediately afterwards the Attackers switch to A_1 being

Runner and A_2 being Penetrator. The Attackers, as the maximizers, receive a significant gain over the equilibrium Value *without knowing what T will do or whether it will suddenly switch*. This is a symptom of the saddle-point property of the equilibrium. However, this example, alone, is far from sufficient to prove that the GSE and SFNE are equivalent everywhere.

VII. CONCLUSION

In this paper, we have introduced the two-Attacker, single-Turret circular target guarding problem. Our focus was on a region of the state space in which neither Attacker can guarantee to reach the target, individually. We considered the case where one Attacker can guarantee to reach the target when the Turret pursues its fellow Attacker. Within this case, we posed and solved a differential game which terminates when the Runner is neutralized, and we posed and solved an optimal control problem for when the Penetrator can reach the target before the Runner is neutralized. Most of the analysis was done under the assumption that Attackers' roles were predefined and that no switching could occur. This assumption was later lifted, and it was shown how the solution already obtained can be used to determine the "best" roles for the Attackers and that this corresponds to the Global Stackelberg Equilibrium.

It remains to formulate and solve a *Game of Degree* in the portion of the state space in which the Turret can guarantee neutralization of both Attackers. Finally, a rigorous proof that the Global Stackelberg Equilibrium and State Feedback Nash Equilibrium are coincident across the state space is left for future work.

ACKNOWLEDGMENT

This paper is based on work performed at the Air Force Research Laboratory (AFRL) *Control Science Center of Excellence*. Distribution Unlimited. 12 Mar 2021. Case #AFRL-2021-0827.

APPENDIX

A. Both Attackers Win

Consider the single-Attacker, single-Turret scenario analyzed in [8], [10]. The region of win for the Attacker, i.e., wherein the Attacker is guaranteed to reach the target circle under optimal play is defined as [10]

$$\mathcal{R}_A \equiv \{(r, \theta) \mid \theta > \theta_{GoK}(r)\}, \quad (47)$$

where

$$\theta_{GoK}(r) = \sqrt{\frac{r^2}{\nu^2} - 1} + \sin^{-1}\left(\frac{\nu}{r}\right) - \sqrt{\frac{1}{\nu^2} - 1} - \sin^{-1}\nu. \quad (48)$$

Lemma 12. *In the two-Attacker, single-Turret scenario with kinematics given by (2), both Attackers are guaranteed to reach the target circle under optimal play, that is, $r_{R_f} = r_{P_f} = 1$ if and only if $A_R, A_P \in \mathcal{R}_A$.*

Proof. Optimal play is given by the respective single-Attacker, single-Turret equilibrium control [8], [10]

$$\sin \psi_i^* = \text{sign}(\sin \theta_i) \left(\frac{\nu}{r_i} \right).$$

The fact that $A_R, A_P \in \mathcal{R}_A \implies r_{R_f} = r_{P_f} = 1$ is due to each Attacker being able to win individually; the presence of additional Attackers does not aid the Turret in any way – both A_R and A_P are able to win. We now prove that $r_{R_f} = r_{P_f} = 1 \implies A_R, A_P \in \mathcal{R}_A$. Suppose $A_i \notin \mathcal{R}_A$, the Turret could choose to implement its one-on-one strategy $u_T = \text{sign}(\sin \theta_i)$ against A_i and be guaranteed to neutralize A_i with $r_i > 1$. \square

B. One or more Attackers Lose

Let the Turret's one-on-one win region be defined $\mathcal{R}_T = \mathcal{R}_A^c$. The trivial case occurs when $A_i \in \mathcal{R}_A$ and $A_j \notin \mathcal{R}_A$ for $i, j \in \{R, P\}$, $i \neq j$. Clearly, A_i can guarantee a win while T can guarantee neutralization of A_j . The construction and solution of a *Game of Degree* in this region of the state space is left for future work.

When $A_R, A_P \notin \mathcal{R}_A$, there is a region of the state space in which one the Attackers can win and a region in which neither can win. The former is analyzed in this paper in detail; the analysis of what the agents should do in the latter region is left for future work.

C. The One-Attacker, One-Turret Differential Game

Lemma 13 (Form of the single-Attacker strategy). *The single-Attacker game, with kinematics $\dot{z} = [\dot{r}_P \ \dot{\theta}_P \ \dot{\beta}]^T$, Value function $V_{AP} = \max_{\psi_P} \min_{u_T} |\theta_{P_f}|$, and terminal surface $\phi = r_{P_f} - 1 = 0$ has an equilibrium the Penetrator strategy of the form*

$$\sin \psi^* = \text{sign}(\sigma_\theta) \frac{\nu}{r_P}. \quad (49)$$

Proof. The Hamiltonian is

$$\mathcal{H} = -\sigma_r \nu \cos \psi_P + \sigma_\theta \left(\frac{\nu}{r_P} \sin \psi_P - u_T \right) + \sigma_\beta u_T, \quad (50)$$

and the adjoint dynamics for the θ_P and β states are

$$\dot{\sigma}_\theta = -\frac{\partial \mathcal{H}}{\partial \theta_P} = 0, \quad \dot{\sigma}_\beta = -\frac{\partial \mathcal{H}}{\partial \beta} = 0. \quad (51)$$

At final time $t = t_f$, the transversality condition yields the terminal adjoint value for the β state

$$\sigma_{\beta_f} = \frac{\partial \Phi}{\partial \beta_f} + \mu \frac{\partial \phi}{\partial \beta_f} = 0, \quad (52)$$

where $\Phi \equiv |\theta_{2_f}|$. Thus $\sigma_\beta = 0$ for all $t \in [0, t_f]$. The Penetrator wishes to maximize the Hamiltonian, while the Turret seeks to minimize it, giving

$$\sin \psi_P^* = \frac{\sigma_\theta}{r_P \sqrt{\sigma_r^2 + \frac{\sigma_\theta^2}{r_P^2}}}, \quad u_T^* = \text{sign}(\sigma_\theta). \quad (53)$$

Substituting (52) and (53) into (50) gives

$$\mathcal{H} = \nu \sqrt{\sigma_r^2 + \frac{\sigma_\theta^2}{r_P^2}} - |\sigma_\theta|. \quad (54)$$

The terminal Hamiltonian value is

$$\mathcal{H}_f = -\frac{\partial \Phi}{\partial t_f} - \mu \frac{\partial \phi}{\partial t_f} = 0. \quad (55)$$

Since the state dynamics are time-autonomous, $\mathcal{H} = 0$ for all $t \in [0, t_f]$. Substituting into (54) and solving for σ_r^2 gives

$$\sigma_r^2 = \frac{\sigma_\theta^2}{\nu^2} - \frac{\sigma_\theta^2}{r_P^2}. \quad (56)$$

Substituting into (53) yields (49). \square

REFERENCES

- [1] U.S. Air Force, "U.S. Air Force 2030 Science and Technology Strategy," tech. rep., 2019.
- [2] R. Isaacs, *Differential Games: A Mathematical Theory with Applications to Optimization, Control and Warfare*. Wiley, New York, 1965.
- [3] Y. Lee and E. Bakolas, "Optimal strategies for guarding a compact and convex target area: A differential game approach," Apr 2021.
- [4] D. Li and J. B. Cruz, "Defending an asset: A linear quadratic game approach," *IEEE Transactions on Aerospace and Electronic Systems*, vol. 47, pp. 1026–1044, 2011.
- [5] K. Margellos and J. Lygeros, "Hamilton-jacobi formulation for reach-avoid differential games," *IEEE Transactions on Automatic Control*, vol. 56, pp. 1849–1861, 8 2011.
- [6] R. Yan, Z. Shi, and Y. Zhong, "Cooperative strategies for two-evader-one-pursuer reach-avoid differential games," *International Journal of Systems Science*, pp. 1–19, 1 2021.
- [7] Z. Akilan and Z. Fuchs, "Zero-sum turret defense differential game with singular surfaces," in *2017 IEEE Conference on Control Technology and Applications (CCTA)*, pp. 2041–2048, 2017.
- [8] D. Shishika and V. Kumar, "Local-game decomposition for multiplayer perimeter-defense problem," in *2018 IEEE Conference on Decision and Control (CDC)*, IEEE, 12 2018.
- [9] D. Shishika, J. Paulos, M. R. Dorothy, M. Ani Hsieh, and V. Kumar, "Team composition for perimeter defense with patrollers and defenders," in *2019 IEEE 58th Conference on Decision and Control (CDC)*, IEEE, 12 2019.
- [10] A. Von Moll, M. Pachter, D. Shishika, and Z. Fuchs, "Guarding a circular target by patrolling its perimeter," in *Conference on Decision and Control*, IEEE, 2020.
- [11] A. Von Moll, M. Pachter, D. Shishika, and Z. Fuchs, "Circular target defense differential games," *Transactions on Automatic Control*, 2021. Submitted for Review.
- [12] M. Pachter, E. Garcia, and D. W. Casbeer, "Active target defense differential game," in *2014 52nd Annual Allerton Conference on Communication, Control, and Computing*, IEEE, 9 2014.
- [13] E. Garcia, D. W. Casbeer, Z. E. Fuchs, and M. Pachter, "Cooperative missile guidance for active defense of air vehicles," *IEEE Transactions on Aerospace and Electronic Systems*, vol. 54, pp. 706–721, 4 2018.
- [14] Z. E. Fuchs, P. P. Khargonekar, and J. Evers, "Cooperative defense within a single-pursuer, two-evader pursuit evasion differential game," in *49th IEEE Conference on Decision and Control (CDC)*, pp. 3091–3097, 2010.
- [15] J. V. Breakwell and P. Hagedorn, "Point capture of two evaders in succession," *Journal of Optimization Theory and Applications*, vol. 27, pp. 89–97, 1979.
- [16] E. Garcia, A. Von Moll, D. Casbeer, and M. Pachter, "Strategies for defending a coastline against multiple attackers," in *IEEE Conference on Decision and Control*, 2019.
- [17] S. Y. Liu, Z. Zhou, C. Tomlin, and K. Hedrick, "Evasion as a team against a faster pursuer," in *2013 American Control Conference*, pp. 5368–5373, 2013.
- [18] O. Hájek, *Toward a general theory of pursuit and evasion*, pp. 143–152. Springer-Verlag, 1977.
- [19] W. M. Getz and M. Pachter, "Capturability in a two-target 'game of two cars'," *Journal of Guidance and Control*, vol. 4, pp. 15–21, 1 1981.
- [20] A. W. Merz, "To pursue or to evade - that is the question," *Journal of Guidance, Control, and Dynamics*, vol. 8, pp. 161–166, 3 1985.
- [21] G. J. Olsder and J. V. Breakwell, "Role determination in an aerial dogfight," *International Journal of Game Theory*, vol. 3, pp. 47–66, 3 1974.
- [22] S. D. Bopardikar, F. Bullo, and J. P. Hespanha, "A cooperative homicidal chauffeur game," *Automatica*, vol. 45, pp. 1771–1777, 2009.

- [23] A. Von Moll, D. Shishika, Z. Fuchs, and M. Dorothy, "The turret-runner-penetrator differential game," in *American Control Conference*, 2021.
- [24] T. Başar and G. J. Olsder, *Dynamic Noncooperative Game Theory*, vol. 160 of *Mathematics in Science and Engineering*. Elsevier, 2nd ed., 1982.
- [25] A. E. Bryson and Y.-C. Ho, *Applied Optimal Control: Optimization, Estimation and Control*. CRC Press, 1975.
- [26] Z. E. Fuchs, E. Garcia, and D. W. Casbeer, "Two-pursuer, one-evader pursuit evasion differential game," in *2018 IEEE National Aerospace and Electronics Conference (NAECON)*, pp. 456–464, IEEE, 2018.
- [27] A. Von Moll, Z. Fuchs, and M. Pachter, "Optimal evasion against dual pure pursuit," in *American Control Conference*, IEEE, 2020.
- [28] E. J. Dockner, S. Jorgensen, N. V. Long, and G. Sorger, *Differential Games in Economics and Management Science* by Engelbert J. Dockner. 2000.
- [29] A. Von Moll, M. Pachter, E. Garcia, D. Casbeer, and D. Milutinović, "Robust policies for a multiple pursuer single evader differential game," *Dynamic Games and Applications*, pp. 202–221, 2019.
- [30] M. J. Osborne, *An introduction to game theory*, vol. 3. Oxford university press New York, 2004.
- [31] J. B. Cruz, "Survey of nash and stackelberg equilibrium strategies in dynamic games," *Annals of Economic and Social Measurement*, vol. 4, 1975.



Michael Dorothy Michael Dorothy received the B.S. degree in aerospace engineering from Iowa State University in 2009 and the Ph.D. degree in aerospace engineering in 2016. He has been an Aerospace Engineer for CCDC Army Research Laboratory since 2015. His research interests include nonlinear dynamics, switched systems, sensitivity-based control, differential game theory, multi-agent collaborative and adversarial planning.



Alexander Von Moll Alexander Von Moll is a researcher with the Control Science Center, Aerospace Systems Directorate, Air Force Research Laboratory. He holds a B.S. in Aerospace Engineering from Ohio State (2012), an M.S. from Georgia Institute of Technology (2016), and Ph.D. in Electrical Engineering from University of Cincinnati (2022). Alex was a Department of Defense SMART Scholar, awarded in 2011 and again in 2014. His research interests include multi-agent systems, cooperative control, and differential games.



Daigo Shishika Daigo Shishika is an assistant professor in the Department of Mechanical Engineering at George Mason University. He obtained his B.S. from the University of Tokyo, Japan, and his M.S. and Ph.D. from University of Maryland, College Park, all in Aerospace Engineering. Before joining George Mason University, Daigo was a postdoctoral researcher in the GRASP laboratory at University of Pennsylvania. His research interest is in the general area of autonomy, dynamics & controls, and robotics.



Zachariah Fuchs Zachariah Fuchs received a B.S. degree in electrical engineering from the University of Evansville in 2007. Subsequently, he was a National Science Foundation Graduate Research Fellow and DoD SMART Scholar at the University of Florida, USA where he received a M.S. and Ph.D. in electrical and computer engineering in 2009 and 2012 respectively. Since 2018, he has served as an Assistant Professor in the Department of Electrical Engineering and Computer Science at the University of Cincinnati.